Analysis and control of Brain Dynamic Models

Lakshmi N Sridhar*

Chemical Engineering Department, University of Puerto Rico, Mayaguez, PR 00681-9046, USA

A B S T R A C T

The nonlinear behavior of the brain's information processing represents one of the key tasks in modern neuroscience, and a lot of research has been conducted in trying to rhythmicity in brain networks. Bifurcation analysis is a powerful mathematical tool used to deal with the nonlinear dynamics of any process. Several factors must be considered, and multiple objectives must be met simultaneously. Bifurcation analysis and multiobjective nonlinear model predictive control (MNLMPC) calculations are performed on two brain dynamic models. The MATLAB program MATCONT was used to perform the bifurcation analysis. The MNLMPC calculations were performed using the optimization language PYOMO in conjunction with the state-of-the-art global optimization solvers IPOPT and BARON. The bifurcation analysis Hopf bifurcation points that lead to limit cycles in the two models. These Hopf points were eliminated using an activation factor that involves the tanh function. The multiobjective nonlinear model predictive control calculations converge to the Utopia point in both the problems, which is the best solution.

Keywords: Bifurcation; Optimization; Control; Neuroscience; Brain; Hopf

Background

Yamaguchi[1] showed that lecticans are organizers of the brain's extracellular matrix. Manor, et al[2]. showed that synaptic depression mediates biostability in neuronal networks with recurrent inhibitory connectivity. Oohashi, et al[3], demonstrated that Bral1, a brain-specific link protein, colocalizes with the versican v2 isoform at the nodes of Ranvier in developing and adult mouse central nervous systems. Bekku, et al[4], performed the molecular cloning of bral2, a novel brain-specific link protein, and demonstrated the immunohistochemical colocalization with brevican in perineuronal nets. Dityatev, et al[5], showed the synaptic plasticity of extracellular matrix molecules. Carulli, et al[6], determined the composition of perineuronal nets in the adult rat cerebellum and the cellular origin of their components.

Rich and Wenner[7] researched sensing and expressing homeostatic synaptic plasticity. Dityatev, et al[8], investigated the activity-dependent formation and functions of chondroitin sulfate-rich extracellular matrix of perineuronal nets. Turrigiano[9] showed that homeostatic signaling was the positive side of negative feedback. Xie, et al[10], demonstrated the existence of Hopf bifurcations in the Hodgkin-Huxley model. Cingolani, et al[11]. investigated the activity-dependent regulation of synaptic AMPA receptor composition and abundance by beta 3 integrins.

Durstewitz[12] discussed the implications of synaptic biophysics for recurrent network dynamics and active memory. Dityatev[13] remodeled the extracellular matrix and epileptogenesis. Kochlamazashvili, et al[14]. showed that the extracellular matrix molecule hyaluronic acid regulates hippocampal synaptic plasticity by modulating postsynaptic l-type ca (2+) channels. Dityatev, et al[15]. demonstrated that the extracellular matrix played a dual role in synaptic plasticity and homeostasis. Dityatev and Rusakov[16] demonstrated the existence of molecular signals of plasticity at the tetrapartite synapse. Wlodarczyk, et al[17]. showed the role played by extracellular

matrix molecules, their receptors, and secreted proteases in synaptic plasticity. Kazantsev, et al[18], developed a homeostatic model of neuronal firing governed by feedback signals from the extracellular matrix.

Soleman, et al[19], investigated the targeting of the neural extracellular matrix in neurological disorders. Dembitskaya, et al[20], studied the effects of enzymatic removal of chondroitin sulfates on neural excitability and synaptic plasticity in the hippocampal CA1 region. Favuzzi, et al[21], investigated the activity-dependent gating of parvalbumin interneuron function by the perineuronal net protein brevican. Jercog, et al[22], demonstrated that the cortical dynamics reflect state transitions in a bistable network. Schmidt, et al[23], showed that the network mechanisms cause oscillations in cognitive tasks. Azeez, et al[24], demonstrated the diurnal fluctuation of extracellular matrix organization in the lateral hypothalamus in basal conditions and in neuroinflammation.

Song and Dityatev[25] investigated the interaction between glia, extracellular matrix and neurons. Lazarevichet al[26] demonstrated the existence of activity-dependent switches between dynamic regimes of extracellular matrix expression. Rozhnova, et al[27] showed the impact of the brain extracellular matrix on neuronal firing reliability and spike-timing jitter. Rozhnova[28] demonstrated the chaotic change of extracellular matrix molecules concentration in the presence of periodically varying neuronal firing rate. Rozhnova, et al[29]. Performed bifurcation analysis calculations on a model of brain extracellular matrix.

This work aims to perform bifurcation and multiobjective nonlinear model predictive control (MNLMPC) on two brain dynamics models, which are Brain extracellular matrix model of Rozhnova, et al[29] and the Hodgkin-Huxley model of Xie, et al[10]. This document is organized as follows. The model equations for both the models are first described. This is followed by a description of the numerical methods (bifurcation analysis and MNLMPC). The results and discussion are then presented, followed by the conclusions.

Brain Dynamics Models

Model 1: Brain extracellular matrix model[29]

The equations in this model are

$$\frac{dzval}{dt} = -(\alpha_z + \gamma_p)zval + \beta_z F_z$$

$$\frac{dpval}{dt} = -\alpha_p pval + \beta_p F_p$$

$$F_z = z_0 - \frac{z_0 - z_1}{1 + \exp(\frac{-Q - \theta_z}{k_z})}$$

$$F_p = z_0 - \frac{p_0 - p_1}{1 + \exp(\frac{-Q - \theta_p}{k_p})}$$

$$Q = Q_0 + \alpha_Q zval$$

The parameter values are

$Q_0 = 5; \alpha_Q = 0.23; \alpha_Z = 0.001; \alpha_p = 0.001; \gamma_P = 0.001; \beta_Z = 0.01;$
$z_0 = 0; z_1 = 1; p_0 = 0; p_1 = 1; k_z = 0.15; k_p = 0.05; \beta_p = 0.01$

zval and pval represent the concentration of the ECM molecules and the concentration of proteases. θ_z, θ_p are the activation midpoints and are the bifurcation and control parameters.

Model 2: Hodgkin-Huxley Model[10]

The equations in this model are

$$\frac{d(vval)}{dt} = \frac{1}{C_M}(I_{EXT} - g_{Na}(mval)^3 hval(vval - vna) - g_K(nval)^4(vval - v_K) - g_L(vval - v_L))$$

$$\frac{d(mval)}{dt} = \alpha_m(1 - mval) - \beta_m(mval)$$

$$\frac{d(hval)}{dt} = \alpha_h(1 - hval) - \beta_h(hval)$$

$$\frac{d(nval)}{dt} = \alpha_n(1 - hval) - \beta_n(hval)$$

Where $\alpha_m, \beta_m, \alpha_h, \beta_h, \alpha_n, \beta_n$ are defined as

$$\alpha_m = 0.1\frac{(25 - vval)}{\{\exp(\frac{25 - vval}{10}) - 1\}}$$

$$\beta_m = 4\exp(-\frac{vval}{18})$$

$$\alpha_h = 0.07\exp(-\frac{vval}{20})$$

$$\beta_h = \frac{1}{\{\exp(\frac{30 - vval}{10}) + 1\}}$$

$$\alpha_n = \frac{0.01(10 - vval)}{\{\exp(\frac{10 - vval}{10}) - 1\}}$$

$$\beta_n = 0.125\exp(-\frac{vval}{80})$$

The parameters are

$V_{Na} = 115.0, V_K = -12.0, V_L = 10.599, g_{Na} = 120.0, g_K = 36, g_L = 0.3, C_M = 1$

vval is the electrical potential difference voltage across the nerve membrane (membrane potential). *mval* and *hval* represent the gating variables for the activation and inactivation of the sodium ion channel, respectively. *nval* is the activation gating variable of the potassium ion channel. I_{EXT} is the external current and the bifurcation and control parameter.

Numerical Procedures

Bifurcation analysis

The MATLAB software MATCONT is used to perform the bifurcation calculations. Bifurcation analysis deals with multiple steady-states and limit cycles. Multiple steady states occur because of the existence of branch and limit points. Hopf bifurcation points cause limit cycles. A commonly used MATLAB program that locates limit points, branch points, and Hopf bifurcation points is MATCONT[30,31]. This program detects Limit points (LP), branch points (BP), and Hopf bifurcation points(H) for an ODE system

$$\frac{dx}{dt} = f(x, \alpha)$$

$x \in R^n$ Let the bifurcation parameter be α Since the gradient is orthogonal to the tangent vector, The tangent plane at

any point $w = [w_1, w_2, w_3, w_4, ... w_{n+1}]$ must satisfy

$$Aw = 0$$

Where A is

$$A = [\partial f / \partial x \quad | \partial f / \partial \alpha]$$

where $\partial f / \partial x$ is the Jacobian matrix. For both limit and branch points, the matrix $[\partial f / \partial x]$ must be singular. The n+1 th component of the tangent vector $w_{n+1} = 0$ for a limit point (LP)and for a branch point (BP) the matrix $\begin{bmatrix} A \\ w^T \end{bmatrix}$ must be singular. At a Hopf bifurcation point,

$$\det(2 f_x(x, \alpha) @ I_n) = 0$$

@ indicates the bialternate product while I_n is the n-square identity matrix. Hopf bifurcations cause limit cycles and should be eliminated because limit cycles make optimization and control tasks very difficult. More details can be found in Kuznetsov[32,33] and Govaerts[34].

Hopf bifurcations cause unwanted oscillatory behavior and limit cycles. The tanh activation function (where a control value u is replaced by) $(u \tanh u / \varepsilon)$ is commonly used in neural nets[35-37] and optimal control problems[38] to eliminate spikes in the optimal control profile. Hopf bifurcation points cause oscillatory behavior. Oscillations are similar to spikes, and the results in Sridhar[39] demonstrate that the tanh factor also eliminates the Hopf bifurcation by preventing the occurrence of oscillations. Sridhar[39] explained with several examples how the activation factor involving the tanh function successfully eliminates the limit cycle causing Hopf bifurcation points. This was because the tanh function increases the time period of the oscillatory behavior, which occurs in the form of a limit cycle caused by Hopf bifurcations.

Mult objective nonlinear model predictive control (MNLMPC)

Flores Tlacuahuaz, et al[40] developed a Mult objective nonlinear model predictive control (MNLMPC) method that is rigorous and does not involve weighting functions or additional constraints. This procedure is used for performing the MNLMPC calculations Here $\sum_{t_{i=0}}^{t_i=t_f} q_j(t_i)$ (j=12..n) represents the variables that need to be minimized/maximized simultaneously for a problem involving a set of ODE

$$\frac{dx}{dt} = F(x, u)$$

t_f being the final time value, and n the total number of objective variables and u the control parameter. This MNLMPC procedure first solves the single objective optimal control problem independently optimizing each of the variables $\sum_{t_{i=0}}^{t_i=t_f} q_j(t_i)$ individually. The minimization/maximization of $\sum_{t_{i=0}}^{t_i=t_f} q_j(t_i)$ will lead to the values q_j^*. Then the optimization

problem that will be solved is

$$\min(\sum_{j=1}^{n}(\sum_{t_{i=0}}^{t_i=t_f} q_j(t_i) - q_j^*))^2$$

$$subject \ to \ \frac{dx}{dt} = F(x, u);$$

This will provide the values of u at various times. The first obtained control value of u is implemented and the rest are discarded. This procedure is repeated until the implemented and the first obtained control values are the same or if the Utopia point where ($\sum_{t_{i=0}}^{t_i=t_f} q_j(t_i) = q_j^*$ for all j) is obtained. Pyomo[41] is used for these calculations. Here, the differential equations are converted to a Nonlinear Program (NLP) using the orthogonal collocation method The NLP is solved using IPOPT[42] and confirmed as a global solution with BARON[43].

The steps of the algorithm are as follows

Optimize $\sum_{t_{i=0}}^{t_i=t_f} q_j(t_i)$ and obtain q_j^* at various time intervals t_i. The subscript i is the index for each time step.

Minimize $(\sum_{j=1}^{n}(\sum_{t_{i=0}}^{t_i=t_f} q_j(t_i) - q_j^*))^2$ and get the control values for various times.

Implement the first obtained control values

Repeat steps 1 to 3 until there is an insignificant difference between the implemented and the first obtained value of the control variables or if the Utopia point is achieved. The Utopia point is when $\sum_{t_{i=0}}^{t_i=t_f} q_j(t_i) = q_j^*$ for all j.

Results and Discussion

For the bifurcation analysis in model 1, both θ_p and θ_z were individually used as bifurcation parameters. When θ_p was used as a bifurcation parameter, two Hopf bifurcation points were found at $(zval, pval, \theta_p)$ values of (2.128943 0.426793 5.645178) and (4.230053 1.696697 6.052311). These Hopf bifurcation points are shown in **(Figure 1a)**. Each of these Hopf bifurcation points result in a limit cycle which are shown in **(Figures 1b and 1c)**. When θ_p was modified to $\frac{\theta_p \tanh(\theta_p)}{1.115}$ the hopf bifurcations disappear **(Figure 1d)**.
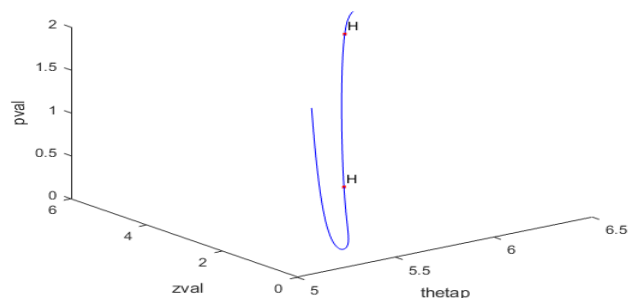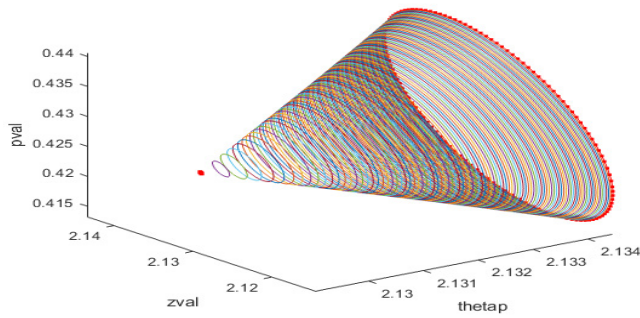

Figure 1a.

Figure 1b.

Figure 1f

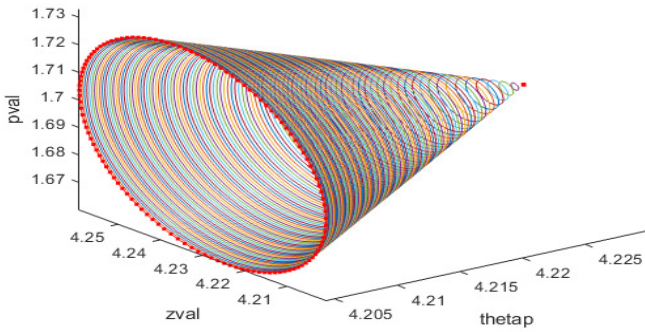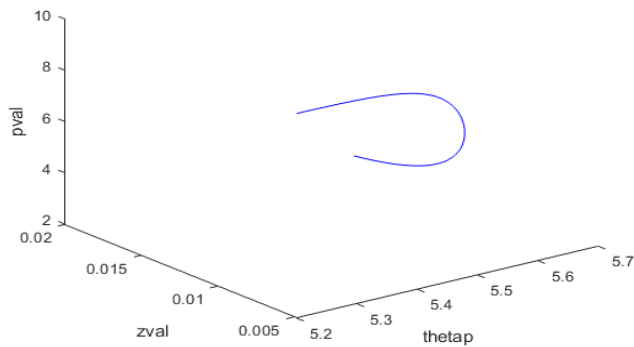Figure 1c.

Figure 1g

Figure 1d.

Figure 1h

When θ_z was used as a bifurcation parameter, two Hopf bifurcation points were found at $(zval, pval, \theta_z)$ values of (2.696435 0.266904 5.951550) and (3.190589 2.102711 5.604739) These Hopf bifurcation points are shown in **(Figure 1e)**. Each of these Hopf bifurcation points result in a limit cycle which are shown in **(Figures 1f and 1g)**. When θ_z was modified to $\dfrac{\theta_z \tanh(\theta_z)}{1.115}$ the hopf bifurcations disappear **(Figure 1h)**.
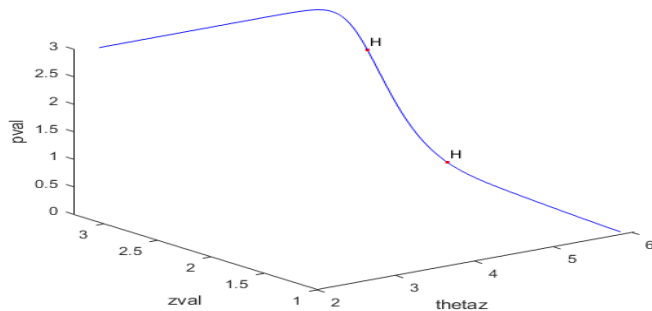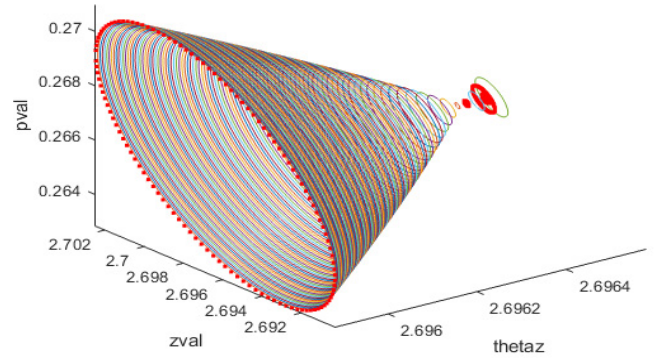
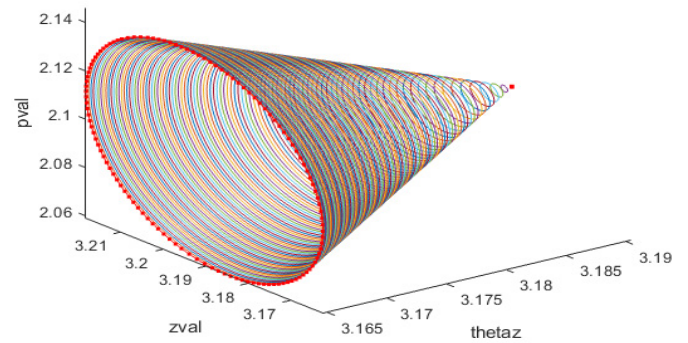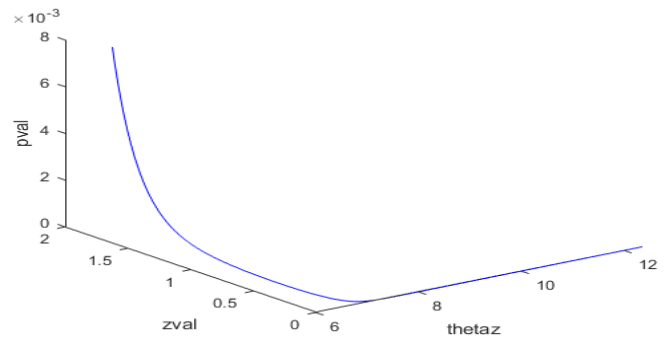

Figure 1e

The MNLMPC calculations were performed using $\dfrac{\theta_p \tanh(\theta_p)}{1.115}$ and $\dfrac{\theta_z \tanh(\theta_z)}{1.115}$ as the control parameters.

$$\sum_{t_{i=0}}^{t_i=t_f} zval_j(t_i)$$ (ECM concentration) was maximized and resulted in a value of 20. $$\sum_{t_{i=0}}^{t_i=t_f} pval_j(t_i)$$ (proteas concentration) was minimized and resulted in a value of 0. The Mult objective optimal control calculation involved a minimization of

$$(\sum_{t_{i=0}}^{t_i=t_f} zval_j(t_i) - 20)^2 + (\sum_{t_{i=0}}^{t_i=t_f} pval_j(t_i) - 0)^2 .$$ This minimization

resulted in the Utopia point (0). The first of the control variables is implemented, and the rest are discarded. The process is repeated until the difference between the first and second values of the control variables are the same. The MNLMPC control values of both θ_p and θ_z were 5 and 5. The zval and pval profiles are shown in **(Figures 1i and 1j)**.
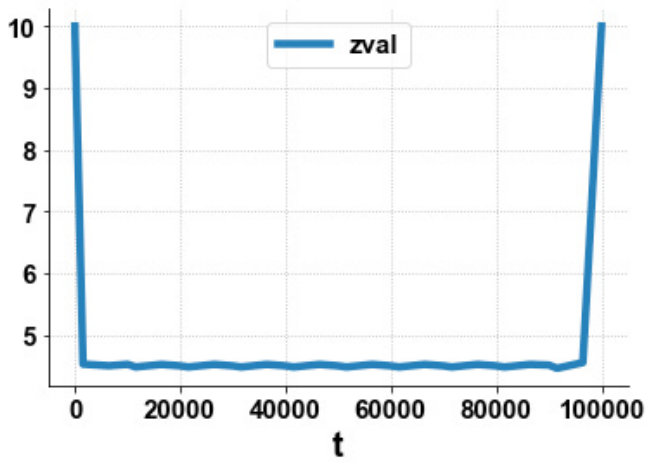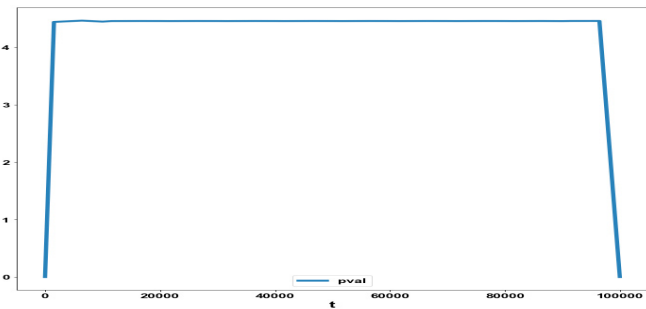
Figure 1i

Figure 1j

In model 2, I_{EXT} is the bifurcation parameter and a Hopf bifurcation point was found at (vval, mval, hval, nval, 2, $_{EXT}$) values of (5.345857 0.097257 0.406228 0.401784 9.779639). This is shown in **(Figure 2a)**. The limit cycle produced by this Hopf bifurcation is shown in **(Figure 2b)**. When I_{EXT} is modified to $\frac{I_{EXT}\ \tanh(I_{EXT})}{1.5}$ the Hopf Bifurcation point disappears.
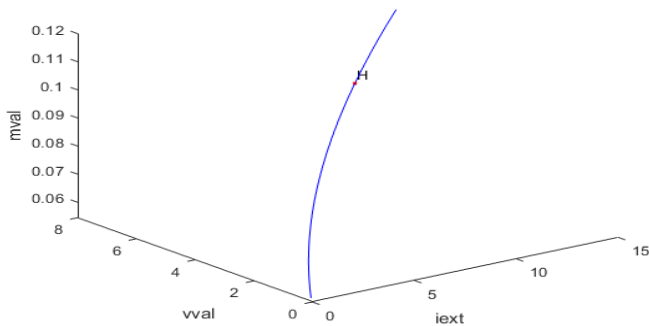

Figure 2a

For the MNLMPC calculations, $\sum\limits_{t_i=0}^{t_i=t_f} vval_j(t_i), \sum\limits_{t_i=0}^{t_i=t_f} mval_j(t_i), \sum\limits_{t_i=0}^{t_i=t_f} nval_j(t_i)$ were maximized and resulted in values of 20,20 and 17.3647. $\sum\limits_{t_i=0}^{t_i=t_f} hval_j(t_i),$ was minimized and resulted in a value of 0.

The multiobjective optimal control calculation involved a minimization of

$$(\sum\limits_{t_i=0}^{t_i=t_f} vval_j(t_i)-20)^2 + (\sum\limits_{t_i=0}^{t_i=t_f} mval_j(t_i)-20)^2 + (\sum\limits_{t_i=0}^{t_i=t_f} nval_j(t_i)-17.3647)^2 + (\sum\limits_{t_i=0}^{t_i=t_f} hval_j(t_i)-0)^2 \cdot$$

$\frac{I_{EXT}\ \tanh(I_{EXT})}{1.5}$ was used as the control parameter.
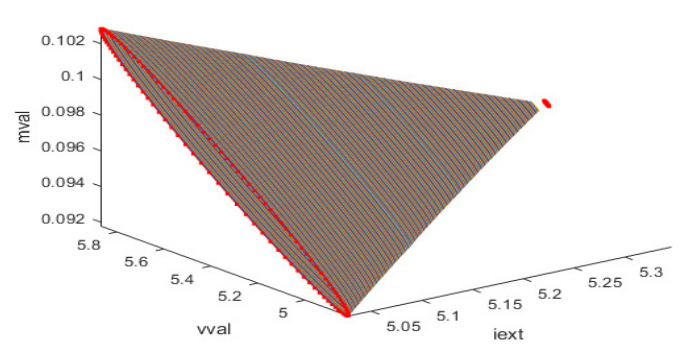

Figure 2b

This minimization resulted in the Utopia point (0). The first of the control variables is implemented, and the rest are discarded. The process is repeated until the difference between the first and second values of the control variables are the same. The MNLMPC control value of I_{EXT} is 1. The vval, hval and nval profiles for the MNLMPC calculations are shown in **(Figures 2d and 2e)**. The mval value was 1 throughout.
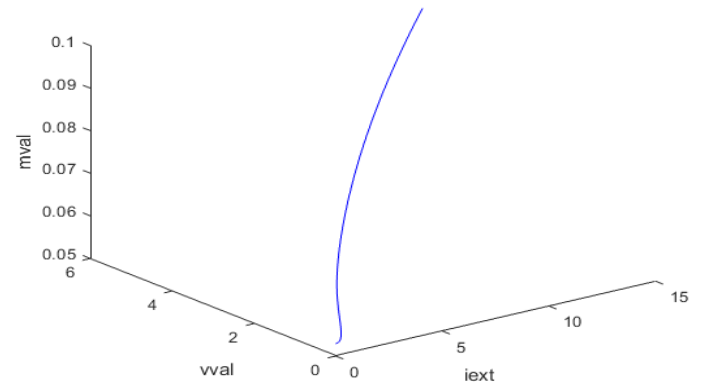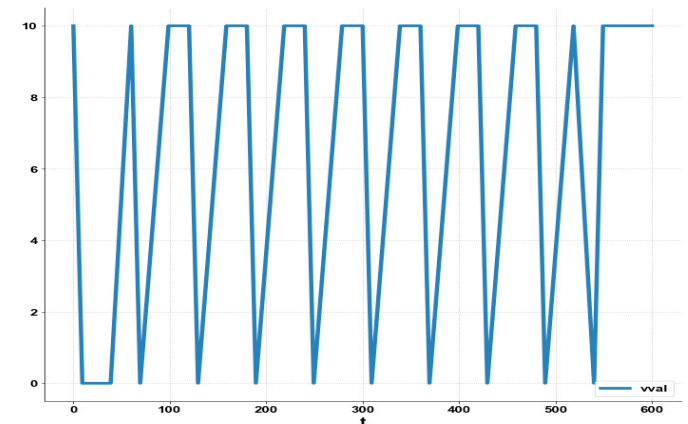

Figure 2c

Figure 2d

Both brain models show the presence of limit cycles causing Hopf bifurcations, which can be eliminated using the activation factor involving the tanh function, confirming the analysis of Sridhar(2024). In both cases, the MNLMPC calculations converge to the Utopia solution.
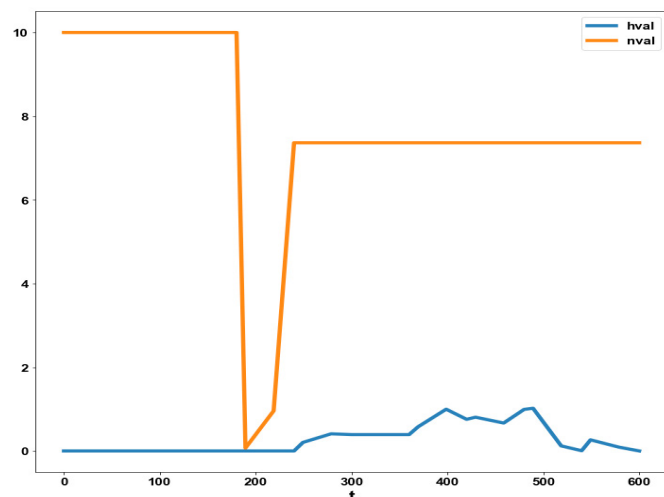
Figure 2e

Conclusion

Multiobjective nonlinear model predictive control calculations were performed along with bifurcation analysis on two models involving brain dynamics. The bifurcation analysis revealed the existence of limit cycle causing Hopf bifurcation points, which are eliminated using an activation factor involving the tanh function. The multiojective nonlinear model predictive calculations converge to the Utopia point(the best possible solution) .in both models.

Data Availability Statement

All data used is presented in the paper.

Conflict of Interest

The author, Dr. Lakshmi N Sridhar has no conflict of interest.

Acknowledgement

Dr. Sridhar thanks Dr. Carlos Ramirez and Dr. Suleiman for encouraging him to write single-author papers.

References

1. Yamaguchi Y. Lecticans: organizers of the brain extracellular matrix. Cellular and Molecular Life Sciences: CMLS 2000;57(2):276-289.

2. Manor Y, Nadim F. Synaptic depression mediates bistability in neuronal net- works with recurrent inhibitory connectivity. J Neurosci 2001;21(23):9460-9470.

3. Oohashi T, Hirakawa S, Bekku Y, et al. Bral1, a brain-specific link protein, colocal- izing with the versican v2 isoform at the nodes of ranvier in developing and adult mouse central nervous systems. Mol Cell Neurosci 2002;19(1):43-57.

4. Bekku Y, Su W-D, Hirakawa S, et al. Molecular cloning of bral2, a novel brain-specific link protein, and immunohistochemical colocalization with brevican in perineuronal nets. Mol Cell Neurosci 2003;24(1):148-159.

5. Dityatev A, Schachner M. Extracellular matrix molecules and synaptic plasticity. Nat Rev Neurosci 2003;4(6):456-468.

6. Carulli D, Rhodes KE, Brown DJ, et al. Composition of perineuronal nets in the adult rat cerebellum and the cellular origin of their components. J Comp Neurol 2006;494(4):559-577.

7. Rich MM, Wenner P. Sensing and expressing homeostatic synaptic plasticity. Trends Neurosci 2007;30(3):119-125.

8. Dityatev A, Brückner G, Dityateva G, Grosche J, Kleene R, Schachner M. Activity-dependent formation and functions of chondroitin sulfate-rich extracellular matrix of perineuronal nets. Dev Neurobiol 2007;67(5):570-588.

9. Turrigiano G. Homeostatic signaling: the positive side of negative feedback. Curr Opin Neurobiol 2007;17(3):318-324.

10. Xie, Yong and Chen, Luonan and Kang, Yan Mei and Aihara, Kazuyuki Controlling the onset of Hopf bifurcation in the Hodgkin-Huxley model. Phys Rev E 2008;7(6).

11. Cingolani LA, Lorenzo A, Thalhammer A, et al. Activity-dependent regulation of synaptic AMPA receptor composition and abundance by beta 3 integrins. Neuron 2008;58(5):749-762.

12. Durstewitz D. Implications of synaptic biophysics for recurrent network dynamics and active memory. Neural Networks 2009;22(8):1189-1200.

13. Dityatev A. Remodeling of extracellular matrix and epileptogenesis. Epilepsia 2010;51(3):61-65.

14. Kochlamazashvili G, Henneberger C, Bukalo O, et al . The extracellular matrix molecule hyaluronic acid regulates hippocampal synaptic plasticity by modulating postsynaptic l-type ca(2+) channels. Neuron 2010;67(1):116-128.

15. Dityatev A , Schachner M , Sonderegger P . The dual role of the extra- cellular matrix in synaptic plasticity and homeostasis. Nat Rev Neurosci 2010;11(11):735-746.

16. Dityatev A, Rusakov D. Molecular signals of plasticity at the tetrapartite synapse. Curr Opin Neurobiol 2011;21(2):353-359.

17. Wlodarczyk J, Mukhina I, Kaczmarek L, Dityatev A. Extracellular matrix molecules, their receptors, and secreted proteases in synaptic plasticity. Dev Neurobiol 2011;71(11):1040-1053.

18. Kazantsev V, Gordleeva S, Stasenko S, Dityatev A. A homeostatic model of neuronal firing governed by feedback signals from the extracellular matrix. PLoS ONE 2012;7(7):e41646.

19. Soleman S, Filippov MA, Dityatev A, Fawcett JW. Targeting the neural extracellular matrix in neurological disorders. Neuroscience 2013;253:194-213.

20. Dembitskaya Y, Song I, Doronin M, Dityatev A, Semyanov A. Effects of enzy- matic removal of chondroitin sulfates on neural excitability and synaptic plas- ticity in the hippocampal CA1 region. 9th FENS Meeting, Milan, Italy 2014:5-9.

21. Favuzzi E, Marques-Smith A, Deogracias R, et al. Activity-dependent gating of parvalbumin interneuron function by the perineuronal net protein brevican. Neuron 2017;95(3):639-655.

22. Jercog D, Roxin A, Barthó P, Luczak A, Compte A, de la RJ. UP-DOWN Cortical dynamics reflect state transitions in a bistable network. Elife 2017;6:e22425.

23. Schmidt H, Avitabile D, Montbrió E, Roxin A. Network mechanisms underlying the role of oscillations in cognitive tasks. PLoS Comput Biol 2018;14(9):e1006430.

24. Azeez IA , Tesoriero C , Scambi I , Mariotti R , Bentivoglio M . Diurnal fluctuation of extracellular matrix organization in the lateral hypothalamus in basal conditions and in neuroinflammation. 11th FENS Forum of Neuroscience, Berlin 2018:7-11.

25. Song I, Dityatev A. Crosstalk between glia, extracellular matrix and neurons. Brain Res Bull 2018;136:101-8.

26. Lazarevich I , Stasenko S , Rozhnova M , Pankratova E , Dityatev A , Kazantsev V . Activity-dependent switches between dynamic regimes of extracellular matrix expression. PLoS ONE 2020;15(1):e0227917.

27. Rozhnova MA , Pankratova EV , Kazantsev VB . Brain extracellular matrix impact on neuronal firing reliability and spike-timing jitter. In: Advances in Neural Computation, Machine Learning, and Cognitive Research III (Part of the Studies in Computational Intelligence book series 2020;856:190-196.

28. Rozhnova MA, Bandenkov DV, Kazantsev VB, Pankratova EV. Chaotic change of extracellular matrix molecules concentration in the presence of periodically varying neuronal firing rate. Communications in Computer and In- formation Science, Mathematical Modeling and Supercomputer Technologies 2021;1413:117-128.

29. Rozhnova MA, Evgeniya V, Sergey VP. Bifurcation analysis of metastability and oscillation emergence in a model of brain extracellular matrix, Chaos, Solitons Fractals 2021;151:111253.

30. Dhooge A, Govearts W, Kuznetsov AY. MATCONT: A Matlab package for numerical bifurcation analysis of ODEs. ACM transactions on Mathematical software 2003;29(2):141-164.

31. Govaerts AW, Kuznetsov YA, Mestrom W, Riet AM. CL_MATCONT: A continuation toolbox in Matlab 2004.

32. Kuznetsov YA. Elements of applied bifurcation theory. Springer NY 1998.

33. Kuznetsov YA. Five lectures on numerical bifurcation analysis. Utrecht University NL 2009.

34. Govaerts WJF. Numerical Methods for Bifurcations of Dynamical Equilibria. SIAM 2000.

35. Dubey SR Singh SK, Chaudhuri BB. Activation functions in deep learning: A comprehensive survey and benchmark. Neurocomputing 2022;503:92-108.

36. Kamalov AF, Safaraliev NM, Cherukuri AK, Zgheib R. Comparative analysis of activation functions in neural networks. *2021 28th IEEE International Conference on Electronics, Circuits, and Systems (ICECS)*, Dubai, United Arab Emirates 2021:1-6.

37. Szandała T. Review and Comparison of Commonly Used Activation Functions for Deep Neural Networks 2020.

38. Sridhar LN. Bifurcation Analysis and Optimal Control of the Tumor Macrophage Interactions. Biomed J Sci Tech Res 2023;53(5).

39. Sridhar LN. Elimination of oscillation causing Hopf bifurcations in engineering problems. J Applied Math 2024;2(4):1826.

40. Flores-Tlacuahuac A, Morales P, Toledo MR. Multiobjective Nonlinear model predictive control of a class of chemical reactors. I & EC research; 2012:5891-5899.

41. William EH, Laird CD, Watson JP, et al. Pyomo - Optimization Modeling in Python. Second Edition 67.

42. Wächter A, Biegler L. On the implementation of an interior-point filter line-search algorithm for large-scale nonlinear programming. Math Program. 2006;106:25-57.

43. Tawarmalani M, Sahinidis NV. A polyhedral branch-and-cut approach to global optimization. Mathematical Programming 2005;103(2):225-249.